Universal Scaling of Linear and Nonlinear Rheological Properties of Semidilute and Concentrated Polymer Solutions

Youngsuk Heo[†,§] **and Ronald G. Larson***[,†,‡]

Macromolecular Science and Engineering Program, and Department of Chemical Engineering, University of Michigan, Ann Arbor, Michigan 48109-2136

Received March 8, 2008; Revised Manuscript Received August 29, 2008

ABSTRACT: Using oscillatory and steady-shear rheometry on polystyrene (PS) solutions in tricresyl phosphate (TCP) with three nearly monodisperse molecular weights at six values of the reduced concentration c/c_e, where c_e is the entanglement concentration, we show that for each value of c/c_e below 2.0 rheological functions are successfully superimposed using de Gennes "blob" scaling laws for the concentration-dependent plateau modulus G_N^0, and the equilibration time $\tau_{e,scaling}$ using the literature value of the solvent-quality exponent $\nu = 0.53$ (Solomon, M. J.; Muller, S. J. *J. Polym. Sci., Polym. Phys.* **1996**, *334*, 181−192). However, once the polymer volume fraction exceeds the "swelling volume fraction" ϕ_s, above which the polymer takes a random walk configuration on all length scales even in a good solvent, this universal scaling breaks down and the polymer conformation appears to be governed by Colby−Rubinstein's scaling laws for Θ solutions. We estimate that all polybutadiene solutions in phenyl octane (a good solvent) from Colby et al. (*Macromolecules* **1991**, *24*, 3873−3882) are above ϕ_s and can be scaled using Θ solvent scaling laws for concentrations ranging all the way up to the melt, showing that the rheological properties of melts and solutions above ϕ_s follow the same universal behavior. In general, using the "blob" model for semidilute solutions and the Colby−Rubinstein scaling for concentrated solutions collapses linear and nonlinear rheological properties for polymer solutions onto universal curves.

1. Introduction

While the rheological properties of both polymer melts and dilute polymer solutions have been extensively studied, the rheology of semidilute polymer solutions has received less attention, even though many commercially useful polymer solutions, such as polyelectrolytes, emulsions, gels, and personal care products, are semidilute. One possible reason for this is that semidilute solutions are "theoretically inconvenient" because for them both polymer−polymer and polymer−solvent interactions need to be considered simultaneously. However, progress can be made using the concept of the excluded volume "blob", or correlation blob, first suggested by Edwards[6] and developed in detail by de Gennes.[1] This model assumes that excluded volume interactions and hydrodynamic interactions are important on length scales smaller than that of the correlation blob in a good solvent, but are screened on larger length scales. Analysis of the relative contributions of thermal energy, excluded volume interactions, and entanglement interactions indicates the existence of four different polymer concentration regimes, each with different concentration scaling laws governing chain configuration and/or dynamics.[7−9] These four regimes are separated from each other by the three transitional concentrations c^*, c_e, and $c_s = \rho_{polymer}\phi_s$, with $\rho_{polymer}$ as the polymer density, which are discussed shortly. While thorough investigations of thermodynamic properties, such as osmotic compressibility measured by light scattering, have been carried out, rheological properties, which are affected by hydrodynamic, frictional, and entanglement interactions, have not been quite as thoroughly studied.[2,7] However, in the early 1980s, Marin et al.[10] were among the first to study the universality of the linear viscoelastic behavior of concentrated polymer solutions and melts. Focusing on the similarity in rheological properties in the low frequency region of the complex moduli, they proposed time-chain length and time−concentration superpositions in plots of $J_N^0G^*$ versus $\eta_0J_N^0\omega$, where J_N^0 is the plateau creep compliance, G^* is the complex modulus, η_0 is the zero-shear viscosity, and ω is the frequency. Here, J_N^0 scales as $1/G_N^0$ with G_N^0 as the plateau modulus, and thus $\eta_0J_N^0$ can be considered to be a measure of the longest relaxation time. These superposition principles suggested that effects of chain length and concentration can be effectively subsumed into the plateau modulus and the relaxation time, which allows one to collapse G' and curves for different molecular weights and concentrations into a universal plot in the low frequency region. Yet these early superposition methods were phenomenological, yielding simple, but unexplained, power−law relationships relating the modulus and time or frequency shift factors to the concentration or molecular weight.

About a decade ago, Raspaud et al.[2] presented a pioneering study of rheological scaling laws based on the "correlation blob" model by de Gennes.[1,11,12] This work drew on a series of seminal papers that used light scattering to demonstrate the need for an additional concentration scaling parameter, the entanglement concentration c_e, besides just the overlap concentration c^*.[13−15] Raspaud et al. measured zero-shear viscosities of three different polymer/solvent pairs and successfully placed almost all of their experimental points on a single master curve of $\eta_0/\eta_{Rouse} = 60 \times (c/c_e)^{3.4}$, where η_0 is the zero-shear viscosity of the polymer solution, η_{Rouse} is the hypothetical Rouse viscosity for an unentangled polymer solution of the same molecular weight, c_e is the concentration at which the entanglement effect begins, and c is the concentration of polymer in weight per unit volume. Expanding on this by using data for 11 additional polymers, Heo and Larson[3,16] created a master curve, which for $c/c_e > 0.5$ yielded a best-fit power law of

$$\eta_p/\eta_{Rouse} = (43 \pm 2) \times (c/c_e)^{3.12\pm0.05} \quad (1)$$

Here, for an entangled semidilute solution, $\eta_p \equiv \eta_0 - \eta_s$ with η_s as the solvent viscosity, $\eta_{Rouse} = \eta_s(c/c_\eta^*)^{1/(3\nu-1)}$, where $c_\eta^* \equiv 1/[\eta]_0$ with $[\eta]_0$ as the intrinsic viscosity, and ν as the excluded volume exponent. The scaling of the Rouse viscosity with concentration is derived below; see especially eq 6. The excluded volume exponent ν appears in the expression for the

* Corresponding author. E-mail: rlarson@umich.edu.
† Macromolecular Science and Engineering Program.
‡ Department of Chemical Engineering.
§ Present address: Abbott Nutrition, 3300 Stelzer Rd., Dept. 104140, Bldg. RP4-2, Columbus, Ohio 43219.

10.1021/ma800521g CCC: $40.75
Published on Web 10/29/2008

Rouse viscosity because the Rouse chain is a string of $N/g = (c/c^*)^{1/(3\nu-1)}$ excluded volume blobs whose size is dictated by ν. In the dilute concentration regime, the polymer contribution to the viscosity is linear in concentration with slope $\eta_s[\eta]_0$, and by definition reaches a value equal to the solvent viscosity at the overlap concentration $c_\eta^* \equiv 1/[\eta]_0$. The entanglement concentration c_e is defined as $c_e \equiv c_A^* n_e^{3\nu-1}$, where $c_A^* \equiv 1/(M_w A_2)$ with M_w as the weight-average molecular weight, A_2 as the second virial coefficient, and n_e as the number of blobs needed for an entanglement.[2,3] The entanglement concentration is defined so that at this concentration, the number of blobs per chain, N/g, is equal to n_e. The overlap concentration based on the second virial coefficient, c_A^*, is proportional to that based on the radius of gyration, $c^* = M_w/(N_A R_g^3)$, where for the polymer/solvent pair considered here, polystyrene in tricresyl phosphate, we take $c^* M_w A_2 = 6.5 \pm 0.2$, which is the value of this product averaged over the values for two polystyrene/benzene solutions.[2] Using this for PS/TCP, we take $c_A^* = c^*/6.5$. We use c_A^* rather than c_η^* or c^* in the definition of c_e, to remain consistent with the methodology of Raspaud et al.[2] This choice, however, only affects the magnitude of c_e and not its scaling with polymer concentration or molecular weight for a given polymer/solvent pair, and thus other choices would not change the conclusions of this Article.

In this Article, we will explore more broadly the dynamic similarity of semidilute polymer solutions at the same value of c/c_e by comparing frequency and shear-rate-dependent viscoelastic properties. We first compare the reduced complex moduli (G'/G_N^0 and G''/G_N^0) against reduced frequency ($\omega\tau_e$) of polystyrene (PS)/tricresyl phosphate (TCP) solutions with the same value of c/c_e. Here, τ_e is the "equilibration time", which is the Rouse time of an entanglement "tube" segment, which we will discuss in more detail below. We then compare the reduced zero-shear viscosity (η_p/η_{Rouse}) and the reduced first normal stress coefficient ($\psi_1/(\eta_{Rouse}\tau_e)$) against reduced shear rate ($\dot{\gamma}\tau_e$) for these solutions, again at constant values of c/c_e.

We will then discuss a transition to the concentrated solution regime, which occurs at concentrations above a "swelling" volume fraction ϕ_s. In addition, we will present a procedure for determining the proportionality coefficient K_1 relating the equilibration time of the Doi−Edwards tube theory for polymer melts,[17] $\tau_{e,DE}$, to the equilibration time derived from the scaling theory for entangled concentrated solutions,[8] $\tau_{e,scaling}$:

$$\tau_{e,DE} = K_1 \tau_{e,scaling} \tag{2}$$

Through this relationship, we can plot the complex moduli of concentrated solutions and melts against the same renormalized frequency $\omega\tau_{e,DE}$ and thereby test whether entangled polymer melts are dynamically equivalent to concentrated solutions.

2. Theory

Self-similarity in molecular conformation is the foundation for the static scaling theory of semidilute polymer solutions. In a semidilute solution, whose concentration exceeds the polymer overlap concentration c^*, the "correlation blob size" ξ can be defined as the distance scale below which a given polymer molecule is more likely to contact itself, due to chain connectivity, than to contact another polymer chain. Thus, the polymer conformation at small length scales, below the correlation blob size, remains the same as in a dilute solution, for which polymer-excluded volume effects are important. Yet, as the length scale expands beyond the size of a single correlation blob, the excluded volume effect is progressively screened by interactions of the chain with other chains. Thus, inside a correlation blob, the polymer coil is swollen in a good solvent, while on length scales larger than the correlation blob, the chain conformation resembles that of a melt, for which excluded volume is screened out. Hence, the chain in a semidilute solution can be thought of as a "melt of correlation blobs" with each correlation blob acting as a rescaled monomer, and the conformation of a chain as a whole follows the random-walk formula, $R^2 \approx (N/g)\xi^2$, with R as the end-to-end distance, N as the number of monomers per chain, and g as the number of monomers per correlation blob.[2,11] Because the dynamics of polymer chains in the dilute regime are governed by the Zimm model,[19] and the portion of the chain inside the correlation blob behaves as though it is in the dilute regime, the longest relaxation time of a polymer chain segment inside a correlation blob τ_{blob} should be:

$$\tau_{blob} \approx \frac{\xi^2}{D_{blob}} \approx \frac{\xi^2}{k_B T/\zeta_{blob}} \approx \frac{\eta_s \xi^3}{k_B T} \tag{3}$$

where the diffusion coefficient and the friction coefficient of a correlation blob are, respectively, $D_{blob} \approx k_B T/\zeta_{blob}$ and $\zeta_{blob} \approx \eta_s \xi$ according to the Stokes−Einstein relation. However, at length scales larger than ξ, excluded volume and hydrodynamic interactions should be screened out by the presence of the other chains, and so, if the chains are not entangled, their behavior should follow the Rouse theory,[20] yielding the longest Rouse relaxation time,

$$\tau_{Rouse} \approx \tau_{blob}(N/g)^2 \tag{4}$$

In the unentangled regime, the elastic shear modulus G_{Rouse} and the Rouse viscosity η_{Rouse} are, respectively:

$$G_{Rouse} \approx \frac{k_B T}{(N/g)\xi^3} \tag{5}$$

and

$$\eta_{Rouse} \approx \eta_s (N/g) \tag{6}$$

As the concentration increases even higher and exceeds the entanglement concentration c_e, the entanglement effect comes into play, and the dynamics of the polymer chains are then controlled by the tube diameter according to the Doi−Edwards tube model.[17] Hence, the tube diameter should be controlled by the size of a correlation blob ξ and the number of correlation blobs per entanglement strand n_e, and because the correlation blob is a renormalized monomer, n_e should be almost the same as the number of monomers per entanglement N_e for the same polymer species in melt state.[2] The Rouse time required for a submolecule large enough to fill one "tube segment" to relax gives the time scale τ_e. Therefore, if these three parameters, n_e, ξ, and τ_e, are determined, we can compare the linear and nonlinear rheology of different semidilute linear polymer solutions by using ξ and n_e to normalize the modulus, and τ_e to normalize the frequency (or shear rate). Here, $n_e\xi^3$ is related to the plateau modulus of a semidilute solution by the classical rubber elasticity theory[18] as

$$G_N^0 \approx k_B T/(n_e \xi^3) \tag{7}$$

Because correlation blobs in semidilute solutions fill the space as do monomers in melts, the volume fraction of polymer in the solution ϕ is equal to the volume fraction of monomers in a single correlation blob of volume ξ^3:

$$\phi \approx g b^3/\xi^3 \tag{8}$$

where b is the statistical segment length, and $\xi \approx b g^\nu$ from the expression for the radius of a coil containing g monomers, while ν is the excluded volume exponent for the polymer/solvent pair. Thus, the above implies that g scales as $\phi^{1/(1-3\nu)}$ and ξ scales as $\phi^{\nu/(1-3\nu)}$, leading to:

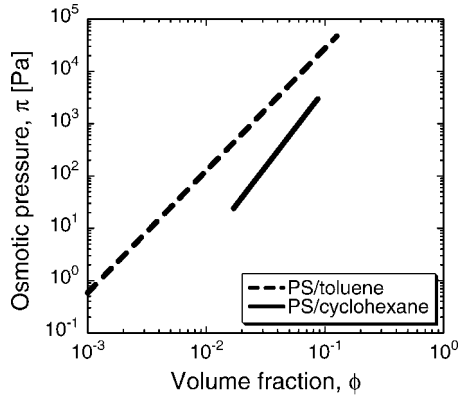

Figure 1. Osmotic pressure for polystyrene (PS) in toluene at 25 °C (a good solvent) and in cyclohexane at the Θ temperature, 35 °C. Dashed lines and solid lines, respectively, denote experimental data of PS/toluene[22] and PS/cyclohexane[21] solutions. Note that the highest volume fraction of PS/toluene is on the order of 0.1, which is presumably smaller than or very close to the swelling volume fraction ϕ_s.

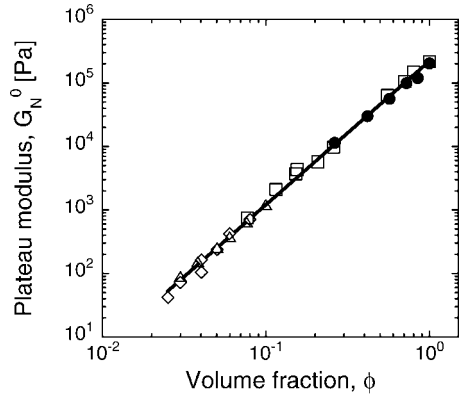

Figure 2. Plateau modulus against volume fraction of nearly monodisperse polystyrene solutions in Aroclor 1248[25,26] (◇ and △), *n*-butyl benzyl phthalate[23] (□), and tricresyl phosphate[24] (●). The line is a least-squares fit to all data.

$$G_N^0(\phi) \approx G_N^0(1)\phi^{3\nu/(3\nu-1)} \tag{9}$$

where $G_N^0(1)$ is the plateau modulus of the melt.

This scaling exponent for G_N^0 is identical to that for the dependence of osmotic pressure π on the volume fraction of a semidilute solution as shown in Figure 1:

$$\pi \sim \phi^{3\nu/(3\nu-1)} \tag{10}$$

Thus, if the modulus follows the same concentration scaling law as the osmotic pressure, the "dilution exponent" α in the relationship $G_N^0 \sim \phi^{1+\alpha}$ should range from 1.31 for good solvents to 2.0 for Θ solvents. However, many experimental measurements on polymer solutions[7,23−27] seem to support the conjecture of Colby and Rubinstein[12] that the "dilution exponent" α in the relationship $G_N^0 \sim \phi^{1+\alpha}$ is 4/3 for Θ solvents. The Colby−Rubinstein conjecture is that the entanglement tube diameter a is proportional to the distance between "binary contacts" of chains in the solution or melt. The concentration of these binary contacts is proportional to ϕ^2, and their separation in three-dimensional space is thus proportional to $\phi^{-2/3}$. Using random-walk statistics, this yields a Colby−Rubinstein dilution exponent of $\alpha = 4/3$ for Θ solvents, which gives no practical difference from the value, $\alpha = 1/(3\nu - 1) = 1.31$ for good solvents with $\nu = 0.588$; see Figure 2. These results, and experimental data on polymer solutions of various solvent qualities, suggest that the dilution exponent α is almost independent of solvent quality. However, note in Figure 2 that many of the experiments that were within the semidilute regime and believed to support the "universality" of the dilution exponent α (such as polystyrene solutions in Aroclor 1248 in Figure 2, for which $\nu = 0.567$) are not useful for exploring the effect of solvent quality on the plateau modulus because they are too close to being in the good-solvent limit ($\nu \cong 0.588$), for which the blob theory gives a dilution exponent of 1.31 ($=1/(3\nu - 1)$), essentially identical to the value proposed for a Θ solvent by Colby and Rubinstein. Thus, for such polymer/solvent pairs, there is no strong difference between the Colby−Rubinstein scaling and the predictions of the blob theory. It is true that there are some solutions studied that have intermediate solvent quality; an example is polystyrene (PS) solutions in tricresyl phosphate (TCP), for which $\nu = 0.53$, and therefore $1/(3\nu - 1) = 1.7$. Although this value of α is different enough from $\alpha = 1.31$ to provide a good test of the de Gennes blob-theory scaling of plateau modulus with concentration, the concentrations studied so far lie mostly outside of the semidilute regime, and are instead within the concentrated regime ($\phi \geq 0.25$; see ● in Figure 2), where the blob theory does not apply. In contrast, the osmotic pressure data of PS/toluene and PS/cyclohexane were all measured within the semidilute regime ($\phi < 0.25$; see solid line in Figure 1), where the de Gennes blob model is supposed to work.

Hence, a thorough test of whether the dilution exponent α is really universal, and independent of both concentration of solvent quality, requires that we measure the dependence of the plateau modulus on polymer concentration in the semidilute (i.e., relatively low concentration) regime using a polymer in a marginally good solvent. We will discuss this further in the Results and Discussion. The characteristic time constant τ_e, which, after the plateau modulus, is the second essential parameter for scaling, corresponds to the Rouse relaxation time of an entanglement strand. We can use eq 4, $\tau_{Rouse} \approx \tau_{blob}(N/g)^2$, to obtain an expression for the equilibration time from the correlation blob relaxation time:

$$\tau_{e,scaling}(\phi) \approx \tau_{blob}[N_e(\phi)/g(\phi)]^2 \approx \frac{\eta_s}{k_B T}\xi(\phi)^3[N_e(\phi)/g(\phi)]^2 \tag{11}$$

where $N_e(\phi)$ is the number of monomers per entanglement strand at volume fraction ϕ, and $N_e(\phi)/g(\phi)$ is essentially equal to n_e,[2] the number of correlation blobs needed for an entanglement. We here append the subscript "scaling" to τ_e because we do not a priori know the order unity coefficient that would be needed to make the scaling relationship, eq 11, into a precise formula for τ_e. Later, we will show how this prefactor may be obtained by relating the above expression to a formula for $\tau_{e,DE}$, the theoretical value of τ_e for entangled melts. In what follows, the generic notation "τ_e" refers to either $\tau_{e,scaling}$ or $\tau_{e,DE}$. Because the radius of gyration of a polymer chain in a dilute solution scales with the number of monomers per chain as $R_g \approx N^\nu$, the correlation blob size ξ at a concentration c above the overlap concentration c^* also follows this relationship $\xi \approx g^\nu$, where $c^* \approx N/R_g^3$ and $c \approx g/\xi^3$. Thus, $c/c^* \approx (g/\xi^3)/(N/R_g^3) \approx (N/g)^{3\nu-1}$ because $\xi/R_g \approx (g/N)^\nu$, leading to $\xi \approx R_g(c/c^*)^{\nu/(1-3\nu)}$. ($R_g$ is the radius of gyration of the polymer in dilute solution, not in semidilute solution.) Therefore, from eq 11, we can write the equilibration time of a semidilute solution in terms of c/c^* as

$$\tau_{e,scaling} = \frac{\eta_s}{k_B T}R_g^3(c/c^*)^{3\nu(1-3\nu)}n_e^2 \tag{12}$$

In the Results and Discussion, we will plot our experimental normalized linear complex moduli, G'/G_N^0, G''/G_N^0 against $\omega\tau_e$, and our experimental nonlinear normalized steady-shear functions, η_p/η_{Rouse}, $\psi_1/(\eta_{Rouse}\tau_e)$ against $\dot{\gamma}\tau_e$, where ψ_1 is the first normal stress coefficient, and $\dot{\gamma}$ is the shear rate.

Table 1. Nominal and Actual Molecular Weights of Polystyrene Samples[a]

vendor	part no. (batch no.)	nominal M_w (10^6 g/mol)	actual M_w (10^6 g/mol)	standard error (10^6 g/mol)
Tosoh Bioscience	F-128	1.09	1.28	0.01
	F-288	2.11	2.53	0.08
	F-550	5.48	6.62	0.06
Polymer Laboratories	20144-13	2.35	2.68	0.06
	20146-15	4.74	5.56	0.10

[a] All weight-average molecular weights were measured with a Wyatt DAWN EOS static light scattering goniometer.

3. Experimental Materials and Methods

3.1. Materials. We purchased nearly monodisperse polystyrene (PS) samples from Tosoh Bioscience and Polymer Laboratories; the part number (batch number) and weight-average molecular weight of each sample are given in Table 1. Tricresyl phosphate (TCP) is used as a marginally good solvent for PS with excluded volume exponent $\nu = 0.53$.[4]

3.2. Sample Preparation. *3.2.1. Weight-Average Molecular Weight Measurements.* We selected six different reduced concentrations within the semidilute regime, $c/c_e = 0.77$, 1.22, 1.65, 1.85, 2.50, and 3.00, where c_e is related to molecular weight through $c_e = c_A^* n_e^{3\nu-1}$, where the overlap concentration here is based on the polymer thermal radius $R_t = [3A_2M_w^2/(16\pi N_A)]^{1/3}$,[3,31] and we define $c_A^* \equiv 1/(M_wA_2) \sim M_w^{1-3\nu}$,[2,3] because R_t is proportional to the radius of gyration[3,32] and the overlap concentration c_A^* scales as M_w/R_t^3. Hence, determining the correct molecular weight is an essential step prior to measurements. Because we use polystyrene samples from two different vendors, we need to check the absolute weight-average molecular weights of these samples using the same device by the same person to ensure consistency. Values of M_w in Table 1 represent the absolute molecular weights measured by small angle static light scattering with a Wyatt DAWN EOS; see Supporting Information.

3.2.2. Preparation of Solutions. We prepared the samples by mixing PS and TCP in dichloromethane (DCM). Even though TCP is a thermodynamically good solvent for PS, dissolving PS in TCP is a kinetically slow process due to relatively high viscosity of TCP (58 cP at 25 °C). For this reason, we use DCM as a cosolvent that helps PS chains dissolve faster by increasing the solvent volume, and by reducing the viscosity of the solution. After complete blending of these three components on a roller overnight, we evaporate most of DCM in a fume hood and completely remove the remaining DCM by placing the samples in a vacuum oven for about 3 weeks until less than 0.001 g of weight loss occurs over 2 consecutive days.

3.2.3. Measuring Rheological Properties with Bubble-Free Samples. We used an ARES LS (Rheometrics) with 25.0 mm diameter parallel plates to obtain the linear and nonlinear viscoelastic properties of semidilute PS/TCP solutions at a temperature of 25.0 ± 0.1 °C controlled using a water bath. Because of the relatively long relaxation times of PS/TCP solutions, when a sample was removed from a container and loaded on the bottom plate of the fixture, air bubbles easily got trapped inside the sample. To remove them, we first placed the bottom plate, on which the sample was loaded, into a vacuum oven and held it at 60 °C for several hours. Next, we applied a vacuum to burst any remaining bubbles. In addition, air bubbles can become trapped in a sample when the upper plate is driven into the sample when setting the gap. Lowering the upper plate faster than the relaxation time of a sample does not give the polymer chains enough time to rearrange themselves under stress, which creates an uneven surface, capturing air between the upper plate and the surface of the sample. Thus, additional care was taken when lowering the upper plate.

4. Results and Discussion

4.1. Nearly Monodisperse Polystyrene Solutions. First, we test the dynamic similarities of semidilute nearly monodisperse polystyrenes (PS) of three different molecular weights in tricresyl phosphte (TCP). Tables 2 and 3 list all necessary parameters for computing the Rouse viscosity $\eta_{Rouse}(\phi)$, the plateau modulus $G_N^0(\phi)$, and the equilibration time $\tau_{e,scaling}(\phi)$ of each solution. Here, $\eta_{Rouse}(\phi)$ is calculated from $\eta_{Rouse}(\phi) = \eta_s(c/c_\eta^*)^{1/(3\nu-1)}$ with $c_\eta^* \equiv 1/[\eta]_0$, where $[\eta]_0$ is the intrinsic viscosity of the polymer.

Table 2. Parameters of Polystyrene (PS)/Tricresyl Phosphate (TCP) Solutions at 25 °C: Zero-Shear Viscosity of TCP η_s, Number of Correlation Blobs per Entanglement for PS/TCP Solutions n_e, Excluded Volume Exponent for PS/TCP Solutions ν, Dilution Exponent α for PS/TCP Solutions, Plateau Modulus of PS Melt at 180 °C $G_N^0(1)$, and Densities of PS and TCP at 25 °C, ρ_{PS} and ρ_{TCP}

η_s Pa·s	n_e[a]	ν[b]	α[c]	$G_N^0(1)$[d] Pa	ρ_{PS} g/L	ρ_{TCP} g/L
0.058	185	0.53	1.7	2.23×10^5	1060	1160

[a] Reference 2. [b] The excluded volume exponent is calculated as $\nu = (a + 1)/3$ from the Mark−Houwink exponent, a in $[\eta]_0 = 4.2 \times 10^{-5}M_w^{0.59}$ (L/g) from data in the molecular weight range of 2×10^5 to 2×10^6 g/mol.[4] We assume that this same excluded volume exponent applies to our samples, including those with molecular weight higher than two million g/mol. [c] α is computed from the relationship, $\alpha = 1/(3\nu - 1)$. [d] $G_N^0(1)$ is calculated from $G_N^0(1) = (4/5)\rho RT/M_e$.[28]

Table 3. Parameters of Polystyrene (PS) of Three Different Molecular Weights in Tricresyl Phosphate (TCP): Weight-Average Molecular Weight M_w, Intrinsic Viscosity $[\eta]_0$, Radius of Gyration R_g, Overlap Concentration c^*, Second Virial Coefficient Multiplied by the Molecular Weight M_wA_2, and Entanglement Concentration c_e of Each PS Sample

M_w g/mol	$[\eta]_0$[a] L/g	R_g[b] nm	c^*[c] g/:	M_wA_2[d] L/g	c_e[e] g/L
1.28×10^6	0.168	43.9	25.2	0.258	84.3
2.53×10^6	0.252	62.9	16.9	0.386	56.4
6.62×10^6	0.444	104.8	9.55	0.680	32.0

[a] $[\eta]_0 = 4.2 \times 10^{-5}M_w^{0.59}$ (L/g).[4] [b] $R_v/R_g = 0.74$ for linear PS solutions over the range $10^5 \le M_w \le 10^{6}$.[31] Here, the viscometric radius of the polymer chain R_v is calculated as $R_v = (\{3[\eta]_0M_w\}/\{10\pi N_A\})^{1/3}$ with N_A as Avogadro's number, and $R_g = (\{3[\eta]_0M_w\}/\{10\pi N_A\})^{1/3}/0.74$.[3] [c] $c^* \equiv M_w/(N_AR_g^3)$. [d] $M_wA_2 = 6.5/c^*$ for PS in good solvents.[2] [e] $c_e \equiv (1/M_wA_2)n_e^{3\nu-1}$.[2,3]

Now, we can compare rheological data of PS/TCP solutions, using $\tau_{e,scaling}$ as a "relative" equilibration time for comparing data for PS/TCP solutions with varying concentration and molecular weight. We measured linear rheological properties for $c/c_e = 0.77$, 1.22, 1.65, 1.85, 2.50, and 3.00, which are tabulated in Table 4 and shown in Figure 3. We were able to measure nonlinear rheological functions for only $c/c_e = 0.77$ and 1.22 due to edge fracture at volume fractions higher than about 10%.[32,33] Even so, for these solutions, excellent superposition is obtained in plots of the nonlinear functions $\psi_1/(\eta_{Rouse}\tau_{e,scaling})$, and η_p/η_{Rouse} against $\dot\gamma\tau_{e,scaling}$, except for low shear-rate regions; see Figure 4. This can be attributed to poor torque values because the lower limit of the transducer (Force Rebalance Transducer, 2K FRTN1 for high range) is 2 g·cm.

In Figure 3, G'/G_N^0 and G''/G_N^0 are plotted against $\omega\tau_{e,scaling}$ for PS of three different molecular weights in TCP at various c/c_e's, ranging from 0.77 to 3.00. At relatively low c/c_e, $c/c_e = 0.77$, 1.22, 1.65, and 1.85, we have excellent collapse with only slight discrepancies in the terminal region. However, the shapes of the G''/G_N^0 curves between the terminal and the high-frequency regions begin to deviate from each other with increasing c/c_e, indicating the gradual breakdown of the universality based on the "blob" model within the semidilute regime. Thus, the superposition of the complex moduli starts to break down when the reduced concentration exceeds $c/c_e = 2.0$ for nearly monodisperse PS/TCP solutions. This breakdown of "universal" scaling for semidilute solutions is also observed with the binary blends of two different molecular weights of PS in TCP, as will be presented below. These findings imply that the definition of the plateau modulus obtained from blob theory and classical rubber elasticity theory, $G_N^0 \approx k_BT/(n_e\xi^3)$

Table 4. Volume Fraction ϕ, Equilibration Time $\tau_{e,scaling}$ Calculated from Eq 12, and Plateau Modulus $G_N^0(\phi) = G_N^0(1)\phi^{1+\alpha}$ for Each PS/TCP Solution at Various Molecular Weights M_w, and Reduced Concentrations c/c_e

nominal $c/c_e = 0.77$						nominal $c/c_e = 1.22$					
M_w g/mol	ϕ	actual c/c_e	$\tau_{e,scaling}$ s	$G_N^0(\phi)$ Pa	η_{Rouse} Pa·s	M_w g/mol	ϕ	actual c/c_e	$\tau_{e,scaling}$ s	$G_N^0(\phi)$ Pa	η_{Rouse} Pa·s
1.28×10^6	0.061	0.77	0.0206	118	3.33	1.28×10^6	0.094	1.18	0.0065	373	6.87
2.53×10^6	0.040	0.76	0.0626	39	3.27	2.53×10^6	0.065	1.22	0.0176	138	7.27
6.62×10^6	0.024	0.78	0.2711	40	3.41	6.62×10^6	0.036	1.20	0.0844	29	7.10

nominal $c/c_e = 1.65$					nominal $c/c_e = 1.85$				
M_w g/mol	ϕ	actual c/c_e	$\tau_{e,scaling}$ s	$G_N^0(\phi)$ Pa	M_w g/mol	ϕ	actual c/c_e	$\tau_{e,scaling}$ s	$G_N^0(\phi)$ Pa
1.28×10^6	0.131	1.65	0.0026	925	1.28×10^6	0.146	1.84	0.0020	1237
2.53×10^6	0.089	1.67	0.0075	324	2.53×10^6	0.098	1.84	0.0058	419
6.62×10^6	0.049	1.63	0.0369	66	6.62×10^6	0.056	1.86	0.0259	94

nominal $c/c_e = 2.50$					nominal $c/c_e = 3.00$				
M_w g/mol	ϕ	actual c/c_e	$\tau_{e,scaling}$ s	$G_N^0(\phi)$ Pa	M_w g/mol	ϕ	actual c/c_e	$\tau_{e,scaling}$ s	$G_N^0(\phi)$ Pa
1.28×10^6	0.199	2.50	0.0009	6398	1.28×10^6	0.239	3.00	0.0005	9547
2.53×10^6	0.133	2.50	0.0025	2632	2.53×10^6	0.160	3.00	0.0016	3937
6.62×10^6	0.075	2.50	0.0117	756	6.62×10^6	0.091	3.00	0.0071	1131

with $\xi \approx R_g(c/c^*)^{\nu/(1-3\nu)}$, can only be used up to a reduced concentration of about $c/c_e = 2.0$ for our solutions, which corresponds roughly to polymer volume fractions higher than about 15%.

This breakdown in de Gennes blob-theory scaling laws occurring at polymer volume fractions higher than about 15% can be ascribed to a transition from the semidilute to the concentrated regime. As explained by Milner,[9] with increasing concentration, the correlation blob size ξ shrinks, eventually down to the size of the "thermal blob" l_s, below which the conformation of polymer chain follows random-walk scaling even in a good solvent, as shown in Figure 1 of Hayward and Graessley[34] and reproduced in Figure 5. The thermal blob size is the length scale at which entropy maximization favors the random walk because the energy associated with excluded volume interactions reaches the thermal energy; see Figure 6. Milner called this length scale "swelling length" because the excluded volume swelling effect sets in above this length. The swelling volume fraction ϕ_s at which the blob size equals the swelling length is estimated using $\phi_s = N_s\Omega_0/l_s^3$, where N_s is the number of monomers in a chain of thermal blob size l_s, and Ω_0 is the volume of a monomer. One can simplify this using the "packing length" l_p, which depends only on polymer stiffness and bulkiness, and is independent of solvent; it is defined as $l_p = N\Omega_0/R^2(N)$. Because $R^2(N_s) = l_s^2 = N_s b^2$, we have $l_p = N_s\Omega_0/(N_s b^2)$, and in turn, we obtain

$$\phi_s = l_p/l_s \tag{13}$$

Note that the weaker is the solvent (i.e., the closer it is to being a Θ solvent), the larger is the swelling length, and the smaller is the swelling concentration. However, because eq 13 is a scaling relationship with an unknown prefactor of order unity,[9] we cannot calculate directly the swelling concentration for PS/TCP. Nevertheless, we note that Milner's calculated value of $\phi_s = 0.24$ for PS/benzene is not too far from the volume fraction (around 0.15) at which we see a breakdown in superposition based on the correlation blob, and we expect the swelling concentration for our system, PS/TCP, to be smaller than that for PS/benzene, because benzene is a better solvent for PS than is TCP. Milner also nicely summarized the proposed concentration scaling relationships for the tube diameter $a(\phi)$, the number of monomers per entanglement $N_e(\phi)$, and the plateau modulus $G_N^0(\phi)$, above and below ϕ_s, respectively, based on the Colby–Rubinstein conjecture for Θ solutions, and de Gennes' blob model for polymer solutions in a good solvent, with the prefactors chosen to match the scaling relationships at the crossover point. (We will give Milner's scaling relationships in the next section.) For our PS/TCP solutions, we do not have enough data above the swelling concentration to test the Colby–Rubinstein scaling behavior. However, other data in the literature allow us to check this scaling behavior above ϕ_s, and so we examine these data in the next section.

4.2. Melt versus Solution Rheology. As alluded to in the previous section, Milner[9] proposed the following crossover between scaling relationships for the tube diameter $a(\phi)$ for concentrated solutions ($\phi_s < \phi \leq 1$) for which Colby–Rubinstein scaling applies, and semidilute entangled solutions ($\phi_e < \phi < \phi_s$), for which de Gennes blob scaling applies, with ϕ_e as the volume fraction corresponding to c_e,

$$a(\phi) = \begin{cases} a(1)\phi^{-\alpha_c/2}, \phi > \phi_s \\ a(1)\phi_s^{-\alpha_c/2}(\phi/\phi_s)^{\nu/(1-3\nu)}, \phi < \phi_s \end{cases} \tag{14}$$

Note that in the semidilute regime ($\phi < \phi_s$), this scaling law for $a(\phi)$ is the same as the de Gennes scaling law for the blob size $\xi(\phi)$. Because for entangled solutions in the semidilute regime, $G_N^0 \approx k_B T/(a^2\xi)$, while the de Gennes scaling is $G_N^0 \approx k_B T/\xi^3$, these two scaling laws are identical in the semidilute regime.

The exponent α_c should take on the value $\alpha_c = 4/3 = 1.33$ in Θ solvents, according to the Colby–Rubinstein conjecture. As Milner notes, however, above the swelling concentration ϕ_s, in any solvent, the polymer configuration is a random walk on all length scales, and hence the Colby–Rubinstein Θ solvent scaling applies for all polymer–solvent systems above ϕ_s, and the dilution exponent α should therefore take on the universal value α_c above ϕ_s. Nevertheless, in what follows we take α_c to be a slightly polymer–solvent system-specific parameter because many experiments have shown values of α_c that differ slightly (by a few percent at most) from 1.33.

We obtain the number of monomers per entanglement at a volume fraction ϕ from Milner,[9]

$$N_e(\phi) = \begin{cases} N_e(1)\phi^{-\alpha_c}, \phi > \phi_s \\ N_e(1)\phi_s^{-\alpha_c}(\phi/\phi_s)^{1/(1-3\nu)}, \phi < \phi_s \end{cases} \tag{15}$$

Here, $N_e(\phi) = M_e(\phi)/M_0$ with M_0 as the monomer molecular weight, and $M_e(\phi) = (4/5)\rho\phi RT/G_N^0(\phi)$.

Thus, the modulus scales as $G_N^0 \propto \phi/N_e \propto \phi^{1+\alpha}$. In the concentrated region, $\phi > \phi_s$, $\alpha = \alpha_c \approx 1.33$, while in the semidilute regime, $\phi < \phi_s$, we recover the de Gennes scaling where $\alpha = 1/(3\nu - 1)$, and $G_N^0 \propto \phi^{3\nu/(3\nu-1)}$. Because the correlation blob size ξ is proportional to $\phi^{\nu/(1-3\nu)}$ within the semidilute regime (below ϕ_s), and the excluded volume effect

(a) Nominal c/c_e =0.77

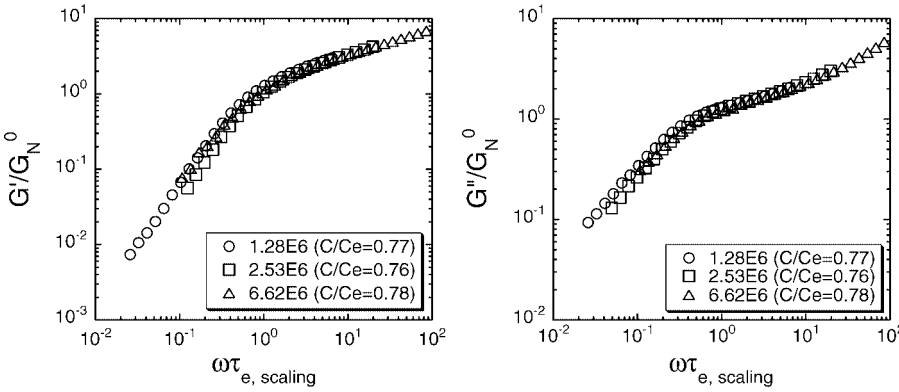

(b) Nominal c/c_e=1.20

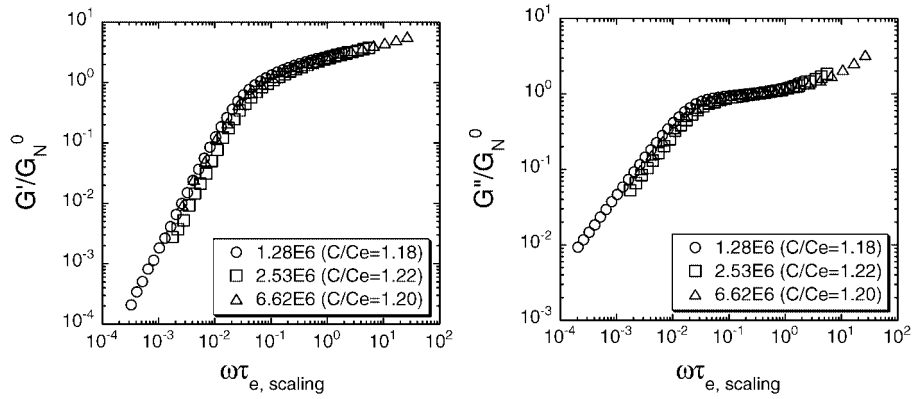

(c) Nominal c/c_e=1.65

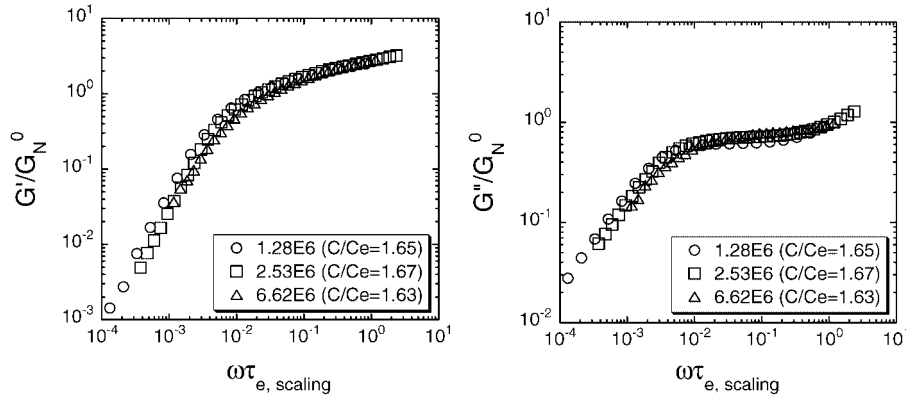

(d) Nominal c/c_e=1.85

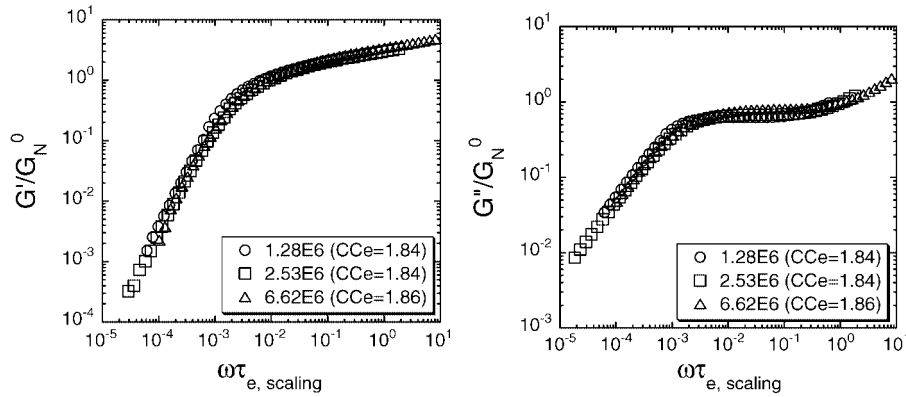

Figure 3. Continued

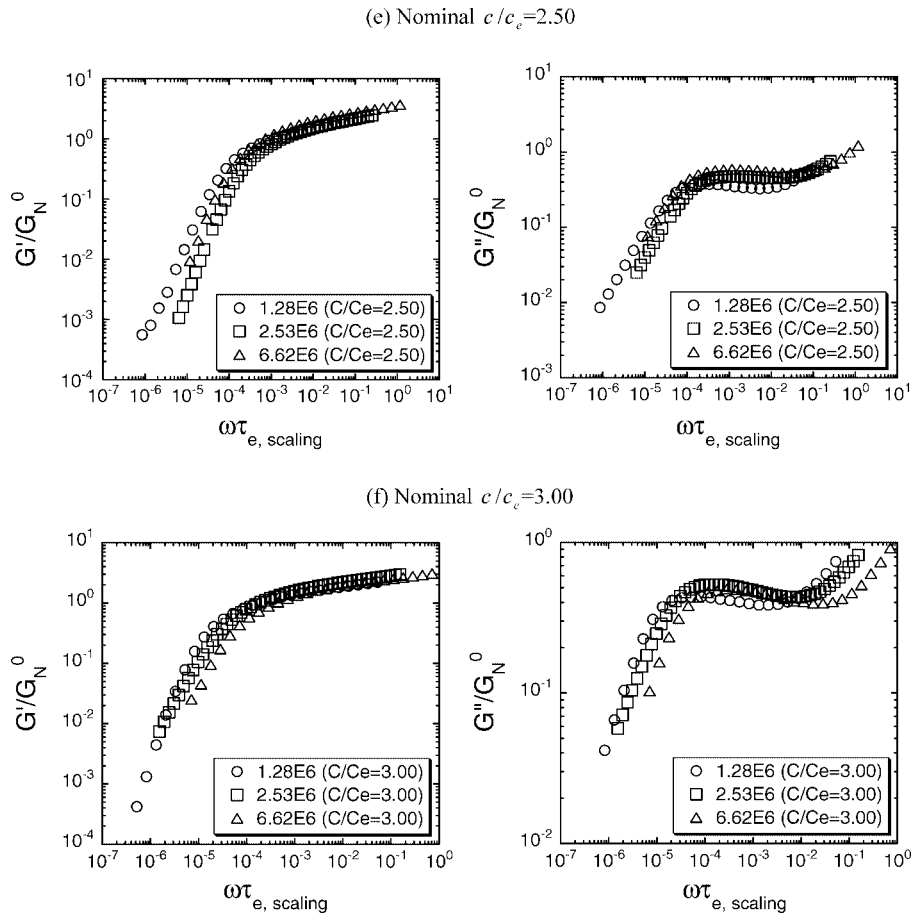

Figure 3. Plots testing "universal scaling" of the linear viscoelastic properties of semidilute monodisperse polystyrene (PS)/tricresyl phosphate (TCP) solutions. In each plot, normalized storage and loss moduli, G'/G_N^0 and G''/G_N^0 are plotted against normalized frequency, $\omega\tau_{e,scaling}$ at a given nominal c/c_e. The small differences in values of c/c_e within each figure are recorded in the legends. ○, □, △, respectively, represent the storage and loss moduli of 1.28×10^6, 2.53×10^6, and 6.62×10^6 g/mol PS solutions.

due to solvent is screened out at any length scale above l_s when the volume fraction goes above ϕ_s, we have

$$\xi(\phi) = \begin{cases} b\phi^{-1}, \phi > \phi_s \\ b\phi_s^{-1}(\phi/\phi_s)^{\nu(1-3\nu)}, \phi < \phi_s \end{cases} \quad (16)$$

and

$$g(\phi) = \phi\xi^3/b^3 = \begin{cases} \phi^{-2}, \phi > \phi_s \\ \phi_s^{-2}(\phi/\phi_s)^{1/(1-3\nu)}, \phi < \phi_s \end{cases} \quad (17)$$

Finally, from eqs 15 and 17, we obtain a formula for the number of blobs per entanglement $N_e(\phi)/g(\phi)$:

$$N_e(\phi)/g(\phi) = \begin{cases} N_e(1)\phi^{2-\alpha_c}, \phi > \phi_s \\ N_e(1)\phi_s^{2-\alpha_c}, \phi < \phi_s \end{cases} \quad (18)$$

Note that the coefficients of the equations are chosen to satisfy continuity of the variables at $\phi = \phi_s$ and $\phi = 1$. For example, at $\phi = 1$, the correlation blob size is equal to the statistical segment length b from $\langle R^2\rangle_0 = Nb^2 = [N(1)/g(1)]\xi(1)^2$, and the number of monomers per blob g is unity.

The above can be summarized as follows. For a very good solvent with $\nu = 0.588$, the dilution exponent below the swelling concentration ϕ_s is $\alpha = 1/(3\nu - 1) \approx 1.31$, while above ϕ_s, the exponent is almost the same, $\alpha = \alpha_c = 1.33$. Thus, for a very good solvent, the dilution exponent is essentially constant across the whole concentration range, as observed experimentally. For a marginally good solvent system, like PS/TCP (for which $\nu = 0.53$), α is larger ($\alpha \approx 1.7$), and α can approach $\alpha = 2$ as the solvent quality approaches Θ quality. However, as the solvent quality worsens, the swelling concentration drops, and the range of concentration over which α can exceed α_c diminishes. When the Θ condition is reached, then the Colby−Rubinstein argument applies for essentially all concentrations above dilute and $\alpha = \alpha_c = 1.33$. Thus, the dilution exponent exhibits a nonmonotonic behavior: for both very good and Θ solvents, α is essentially constant at a "universal value" of around 1.3−1.33 over the entire concentration range, while for marginally good solvents, the exponent is higher than this at low polymer concentrations only. If we start at some intermediate solvent quality and worsen the quality, the magnitude of the deviation in the exponent at low concentrations from the "universal value" increases, but the range of concentrations over which this deviation occurs shrinks to zero as the solvent quality is worsened toward the Θ condition. On the other hand, if we increase the solvent quality, the range of concentrations over which there is a deviation from the "universal exponent" increases, while the deviation itself shrinks nearly to zero when the solvent becomes very good. Thus, the same scaling behavior is reached at both end points (Θ and very good solvent quality), but in different ways. This rather subtle, and nonintuitive, behavior, which is schematically demonstrated in Figure 7, has led to confusion in the literature regarding whether the dilution exponent has a universal value for all polymer/solvent pairs over all concentrations.

We made efforts to use the crossover formulas eqs 16−18 to superpose our PS/TCP data from above the swelling concentration ϕ_s with those below this concentration, by guessing values of ϕ_s. However, the superpositions were not very successful. This is not too surprising because the crossover

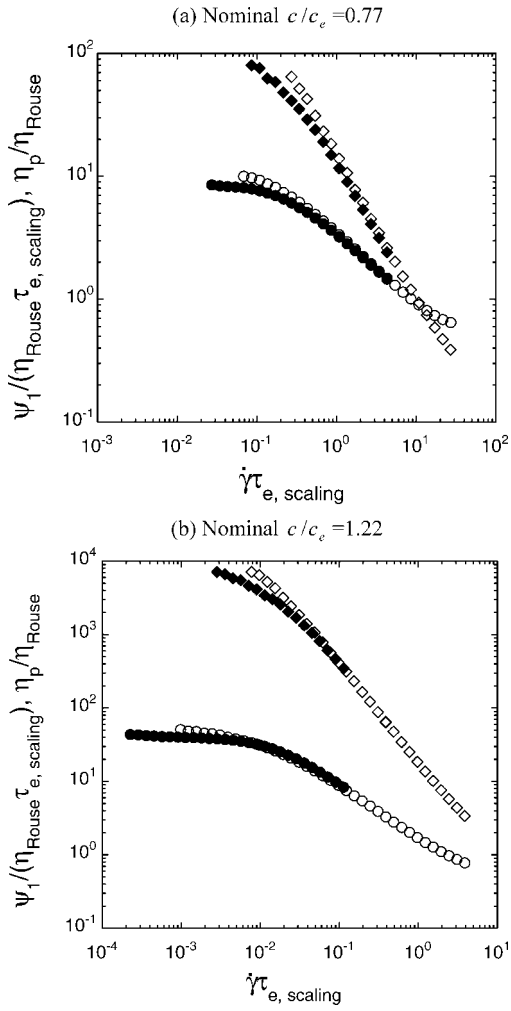

Figure 4. "Universal scaling" of the nonlinear viscoelastic properties of semidilute monodisperse PS/TCP solutions. The normalized first normal stress coefficient $\psi_1/(\eta_{Rouse}\tau_{e,scaling})$ and the normalized steady-shear viscosity η_p/η_{Rouse} are plotted against the normalized shear rate, $\dot{\gamma}\tau_{e,scaling}$, at two nominal values of c/c_e, where the Rouse viscosities for these two concentrations are computed from $\eta_{Rouse} = \eta_s(c[\eta]_0)^{1/(3\nu-1)}$ as given earlier in this section, and are tabulated in Table 4. ◇ and ◆, respectively, represent the normalized first normal stress difference coefficients of 6.62×10^6 and 2.53×10^6 g/mol PS solutions. ○ and ●, respectively, represent the normalized steady-shear viscosities of 6.62×10^6 and 2.53×10^6 g/mol PS solutions.

may not be sharp and because for PS/TCP at the higher concentrations above ϕ_s the glass transition temperature is likely to shift, making our scaling formula for τ_e inaccurate.

4.2.1. Nearly Monodisperse 1,4-Polybutadiene Melts and Solutions in Phenyl Octane. In principle, once the reduced concentration c/c_e exceeds unity, the solution is entangled, and the blob theory for a semidilute polymer solution or the Colby−Rubinstein scaling for a concentrated polymer solution implies that such a solution should be "dynamically equivalent" to a melt having the "same" entanglement density. For semidilute or concentrated entangled solutions, the degree of entanglement can be measured by the ratio c/c_e, while for melts, it is usually measured by the ratio, M/M_e (or N/N_e) of the molecular weight M to the molecular weight between entanglements M_e. We will call this latter ratio the "entanglement density" and will show in what follows that it can also be defined for semidilute solutions, once the dilution exponent is determined. In addition to establishing a common measure of entanglement density for solutions and melts so that "dynamically equivalent" entangled solutions or melts can be identified,

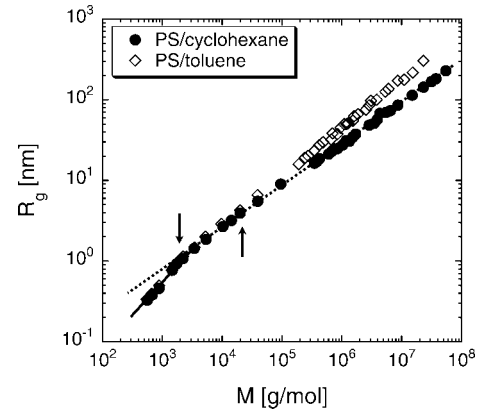

Figure 5. The radius of gyration of dilute polystyrene in a Θ solvent and in a good solvent (reproduced from ref 34). ● and ◇, respectively, represent polystyrene in cyclohexane at Θ temperature (35 °C) and in toluene; dashed line denotes $R_g \sim M^{1/2}$. Even in a good solvent, a polystyrene chain takes Gaussian random walk on a length scale below the swelling length l_s (marked with an upward arrow). As the molecular weight becomes even shorter than the Kuhn length b_K (marked with a downward arrow), polystyrene in any solvent turns into a rigid rod; the solid line denotes $R_g \sim M$.

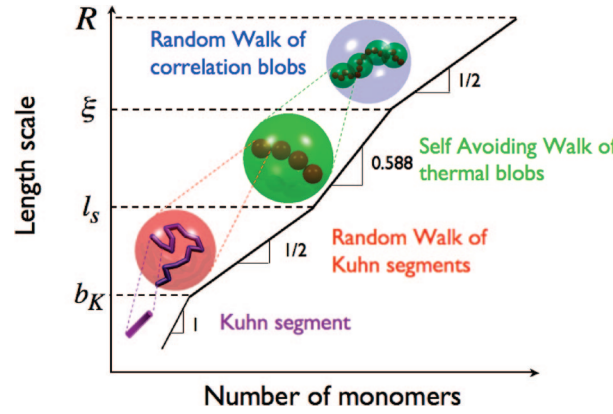

Figure 6. A schematic diagram of the polymer chain length scale with its number of monomers in a very good solvent ($\nu = 0.588$). R, ξ, l_s, and b_K, respectively, represent the end-to-end distance, the correlation blob size, above which excluded volume interactions and hydrodynamic interactions are canceled out, the swelling length, a length scale below which thermal fluctuations dominate over excluded volume interaction, and the Kuhn length.

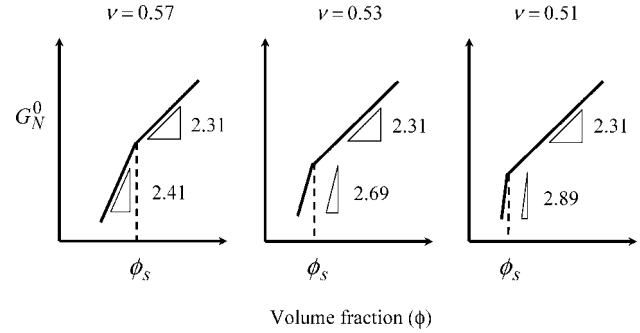

Figure 7. Schematic of the scaling of plateau modulus $G_N^0(\phi)$ of polymer solutions with three different excluded volume exponents, $\nu = 0.57$, 0.53, and 0.51, versus volume fraction ϕ. See text for detail.

the frequency and modulus must be appropriately rescaled, so that data for both solutions and melts can be plotted using common reduced variables.

With this in mind, we now examine an extensive set of data for nearly monodisperse 1,4-polybutadiene solutions in phenyl

octane (PhO) and melts of 1,4-polybutadiene (PBd) of various molecular weights, published by Colby et al.[5] To plot these data on a universal scale, we use the parameters for PBd melts that Likhtman and McLeish[28] determined by fitting the data of PBd melts at 28 °C of Baumgaertel et al.[35] with the Likhtman−McLeish (LM) theory. They thereby determined the values $G_N^0 = 1.47 \times 10^6$ Pa, $M_e = 1.93 \times 10^3$ g/mol (note that M_e was used as an independent fitting parameter, not calculated from $M_e = (4/5)\rho RT/G_N^0$), and $\tau_{e,DE} = 4.9 \times 10^{-7}$ s. Here, we have shifted slightly $\tau_{e,DE}$ at 28 °C to the value $\tau_{e,DE} = 5.66 \times 10^{-7}$ s at 25 °C using the WLF equation with the parameters $C_1 = 3.48$, $C_2 = 163$ K, and $T_0 = 25$ °C.[5] The plateau modulus of a PBd/PhO solution at 25 °C scales as follows:

$$G_{N,PBd}^0(\phi) = G_{N,PBd}^0(1)\phi^{2.29} \tag{19}$$

This scaling relation was determined from experimental measurements of the plateau modulus of PBd/PhO solutions against volume fraction.[5]

Because the glass transition temperature of this solution at any volume fraction is at least 100 K lower than the experimental temperature 298 K, we can use the Fox equation $1/T_g(\phi) = \phi/T_{g,polymer} + (1 - \phi)/T_{g,solvent}$. Here, the glass transition temperature of bulk PBd is $T_{g,PBd} = 174$ K and that of PhO is $T_{g,PhO} = 152$ K. Thus, the glass transition temperatures of the solutions are in the narrow range between 152 and 174 K, well below the temperatures at which the measurements were made (25 °C), and thus the polymer has a similar monomeric friction coefficient in all solutions and the melt. Colby et al.[5] were able to obtain complex moduli of PBd/PhO solutions ($M_w = 925\,000$ g/mol, $M_w/M_n < 1.1$, and 50% cis 1,4, 42% trans 1,4, and 8% vinyl) at various volume fractions from 0.03 up to unity. The swelling volume fraction ϕ_s for PBd/PhO solutions can be bounded from above by the value found for PBd in the good solvent cyclohexane, which is 0.045. Note that PhO is a poorer solvent than cyclohexane for PBd ($\nu = 0.609$ for PBd/cyclohexane,[9] while $\nu = 0.554$ for PBd/PhO[5]), implying that PBd/PhO solution has a longer swelling length, and in turn smaller swelling volume fraction ($\phi_s = l_p/l_s$), than does PBd/cyclohexane because the packing length is independent of solvent quality. From this, we estimate that ϕ_s for PBd/PhO solutions should be significantly less than 0.045. Therefore, we can safely treat all PBd/PhO solutions of Colby et al.[5] as concentrated solutions with $\nu = 0.5$ and $\alpha = 1.29$. This is a remarkable fact for polybutadiene solutions. Even though many researchers[7,36,37] have demonstrated that the dilution exponent of PBd solutions in marginally good to good solvents is independent of solvent quality in seeming contradiction to de Gennes' scaling theory, it turns out that this is not because there is no difference in dilution exponent between good solvent and Θ solvent within the semidilute regime, but instead is because the volume fractions of almost all PBd solutions studied actually belong to the concentrated regime, not the semidilute regime. For polystyrene solutions, where ϕ_s is much larger (around 0.15−0.25), the volume fractions used in our studies presumably cover both semidilute and concentrated regimes. Consistent with this, we showed in the last section that the de Gennes' scaling law collapses our PS/TCP data in the semidilute regime, where we used a dilution exponent of $\alpha = 1.7$, based on the excluded volume exponent, rather than the exponent near 1.3, while superposition based on the exponent $\alpha = 1.7$ gradually breaks down with increasing volume fraction.

To relate $\tau_{e,scaling}$, which is given by the scaling relationship in eq 12 for solutions, to $\tau_{e,DE}$, which is the equilibration time of the Doi−Edwards theory, at a volume fraction that lies in concentrated regime, we take advantage of the fact that Colby et al.[5] obtained both PBd melt and solution data at the same temperature of 25 °C. Thus, we can match the formula for $\tau_{e,DE}$ for a PBd melt to that for a PBd solution simply by setting the "solution" volume fraction to $\phi = 1$, and requiring the two formulas to give the same answer. We use the value of $\tau_{e,DE}$ of a PBd melt that Likhtman and McLeish obtained by fitting their model (the Likhtman−McLeish (LM) model) to the experimental melt data of Baumgaertel et al.[36] by LM model,[28] giving $\tau_{e,DE} = 5.66 \times 10^{-7}$ s. Now, we can obtain $\tau_{e,scaling}(\phi)$ for a PBd solution with the volume fraction ranging $\phi_s < \phi \leq 1$ from eqs 11, 16, and 18:

$$\tau_{e,scaling} = \frac{\eta_s}{k_B T}\xi^3[N_e(\phi)/g(\phi)]^2 = \frac{\eta_s}{k_B T}b^3 N_e^2(1)\phi^{1-2\alpha_c} \tag{20}$$

Comparing $\tau_{e,DE} = 5.66 \times 10^{-7}$ s and $\tau_{e,scaling}(1) = 8.56 \times 10^{-8}$ s thus gives us the prefactor $K_1 = 6.62$ in $\tau_{e,DE} = K_1 \cdot \tau_{e,scaling}$ for this particular polymer/solvent pair without adjustable parameters. Because we have a series of G' and G'' curves for PBd melts and solutions available, we are now able to compare these functions for varying M/M_e for melts and solutions, plotted as: G'/G_N^0, G''/G_N^0 versus $\omega\tau_{e,DE}$. $\tau_{e,DE}(\phi) = K_1 \cdot \tau_{e,scaling}(\phi)$ and $G_N^0(\phi)$ are tabulated in Table 5, and the plots are shown in Figure 8, with filled symbols representing melts and open symbols solutions.

Table 5. Equilibration Times and Plateau Moduli of a Series of PBd/PhO Solutions ($M_w = 9.25 \times 10^5$ g/mol)[a]

ϕ	$N/N_e(\phi)$	$K_1 \cdot \tau_{e,scaling}(\phi)$ s	$G_N^0(\phi)$ Pa
0.021	3.4	7.03×10^{-4}	2.58×10^2
0.027	4.6	3.82×10^{-4}	4.50×10^2
0.062	13.3	5.19×10^{-5}	2.83×10^3
0.140	37.9	7.88×10^{-6}	1.76×10^4
0.280	92.8	1.82×10^{-6}	8.39×10^4
0.488	184.1	7.15×10^{-7}	2.93×10^5
1.000	479.3	5.66×10^{-7}	1.47×10^6

[a] Here, we employ $N_e(\phi) = N_e(1)\phi^{-\alpha_c}$ to compute the number of monomers per entanglement at a volume fraction ϕ.

Note in Figure 8a that treating all solutions and melts as "concentrated solutions" using the scaling exponent $\alpha = \alpha_c = 1.29$ puts all data (melts and solutions) into a simple progression. As $N/N_e(\phi)$ increases, either because of increased molecular weight of increased concentration (and therefore lower $N_e(\phi)$), the transition to terminal behavior occurs at a lower reduced frequency. Note also that a melt and a solution with almost the same value of $N/N_e(\phi)$ (■ and □) have almost identical G' and G'' curves. Unlike PS/TCP solutions, for PBd/PhO solutions a single scaling relationship for the dependence of the plateau modulus on ϕ, $G_N^0(\phi) = G_N^0(1)\phi^{2.29}$ is observed to hold at volume fractions from 100% down to 3%.[5] However, treating all solutions as semidilute solutions, with $\alpha = 1/(3\nu - 1) = 1.51$, does not align the moduli of solutions and melts in a proper sequence as illustrated in Figure 8b. Note that the loss moduli of PBd/PhO solutions show a slight indication of an "early" upturn at high frequencies, which is not present in the melt. If real, and if the "early" upturn continues at higher frequencies, then there may be a significant and unexplained difference between solutions and melts at high frequency.

From the data of Figure 8a, we can extract a reduced crossover frequency, $\omega_X\tau_{e,DE}$, by extrapolating the data for G'/G_N^0 and G''/G_N^0 in the terminal region where $G' \propto \omega$ and $G'' \propto \omega^2$ up to the reduced frequency where G'/G_N^0 crosses G''/G_N^0. From the crossover frequencies of a series of PBd solutions, we get a scaling relationship between the reduced crossover relaxation time, $\tau_X/\tau_{e,DE} = 1/(\omega_X\tau_{e,DE})$, and N/N_e; see Figure 9.

Figure 9 shows us the similarities between melts and solutions. The best-fit power-law slope of the line for melts is 3.27 ± 0.09, and that for solutions is 3.09 ± 0.05, which suggests that, almost to within experimental error, an entangled concentrated solution is essentially the same as a "melt of correlation blobs".

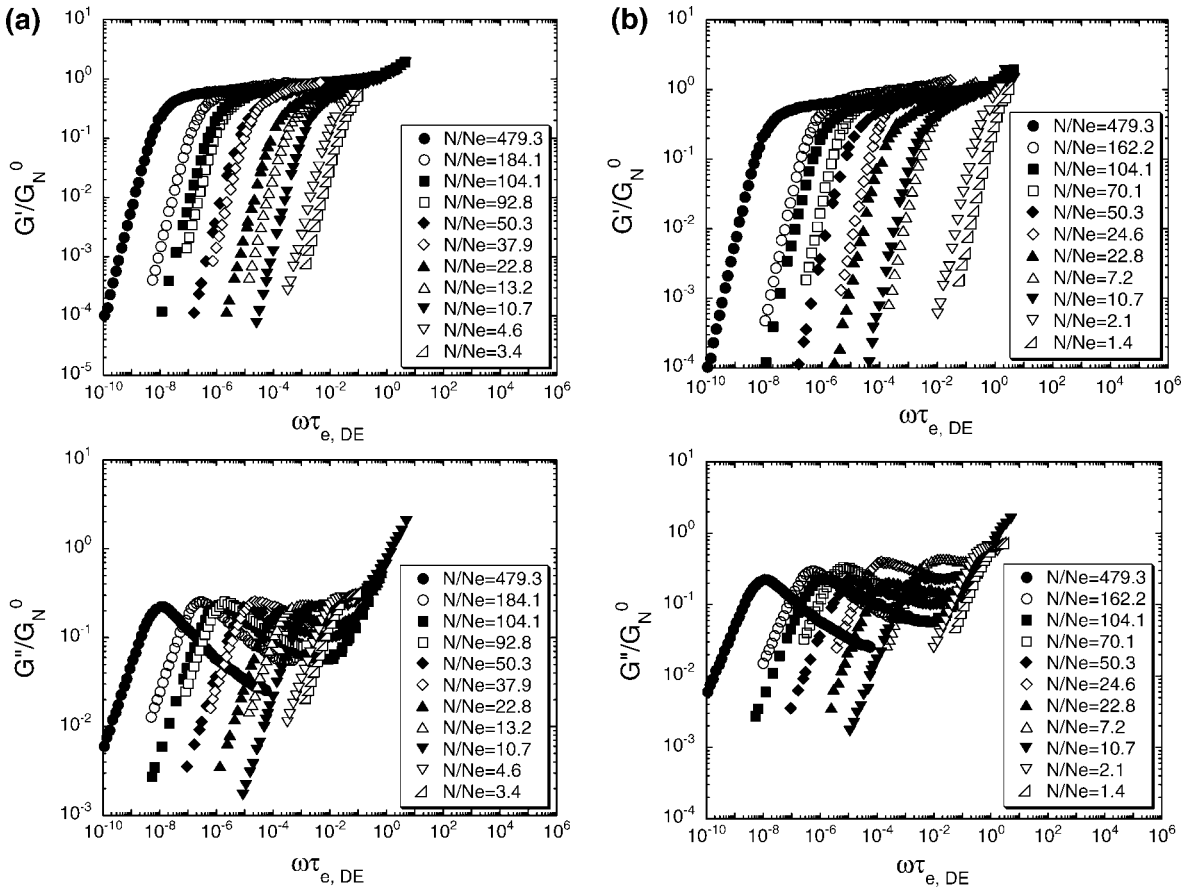

Figure 8. Normalized complex moduli, G'/G_N^0 and G''/G_N^0 against normalized frequency, $\omega\tau_{e,DE}$, for nearly monodisperse polybutadiene (PBd) melts and solutions. Here, $\tau_{e,DE}$ for PBd solutions is computed from $\tau_{e,DE} = K_1 \cdot \tau_{e,scaling}$ with $K_1 = 6.62$, and $N_e(1) = 35.7$. (a) Colby−Rubinstein scaling result using eq 20 with $\alpha_c = 1.29$ (see Table 5), and (b) de Gennes scaling result with $\nu = 0.554$. Filled symbols denote G'/G_N^0 and G''/G_N^0 for PBd melts with $M_w = 9.25 \times 10^5$, 2.01×10^5, 0.97×10^5, 0.44×10^5, and 0.21×10^5 g/mol,[36] and open symbols denote PBd solutions with $M_w = 9.25 \times 10^5$ g/mol at volume fractions of 0.488, 0.280, 0.140, 0.062, 0.027, and 0.021.[5]

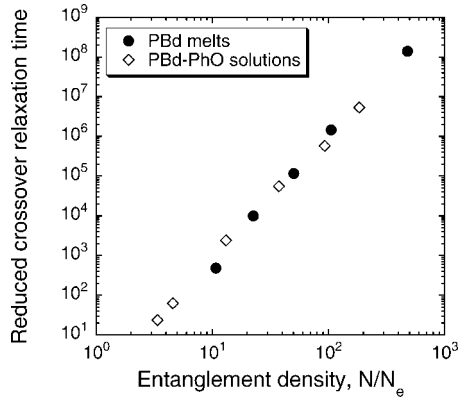

Figure 9. The reduced crossover relaxation time of polybutadiene (PBd) melts and PBd/phenyl octane (PhO) solutions versus the number of entanglements per molecule: N/N_e for melts and solutions. Here, we employ $M_e(1) = 1.93 \times 10^3$ g/mol from Likhtman and McLeish[28] to obtain $N_e(1) = M_e(1)/M_0$, with $M_0 = 54$ g/mol as the monomer molecular weight of PBd. For solutions, we use the scaling law $N_e(\phi) = N_e(1)\phi^{-\alpha_c} = (1.93 \times 10^3/54)\phi^{-1.29}$. ● represent PBd melts (N/N_e = 10.7, 22.9, 50.3, 104.2, and 479.3), and ◇ represent PBd/PhO solutions of $M_w = 9.25 \times 10^5$ (N/N_e = 3.4, 4.6, 13.3, 37.9, 92.8, 184.1, and 479.3).

4.3. Extension to Binary Blends. Most synthetic polymers have broad molecular weight distributions, and some polydispersity is inevitable even when synthesizing nearly monodisperse linear polymers through anionic polymerization. Because polydisperse systems are both more common and more relevant commercially, we would like to encompass polydispersity within the "universal scaling" law.

Binary blends of monodisperse polymers provide a first step to confirm the validity of the "blob" model scaling for polydisperse polymer solutions. Comparing both linear and nonlinear rheological responses of one binary blend with another having the same ratio of short- to long-chain molecular weight and the same c/c_e should determine the validity of the universal scaling for polydisperse semidilute solutions that are not monodisperse. Here, we base c/c_e on the weight average molecular weights of the short and long chains, each of which occupies 50 wt % of the polymer; see Table 6.

As illustrated in Figures 10 and 11, two binary blends with almost the same ratio of short- to long-chain molecular weight and the same c/c_e show excellent agreement in both linear and nonlinear rheological responses with exceptions for $c/c_e = 2.50$ and 3.00, just as was the case for monodisperse PS/TCP solutions. This allows us to further extend the universal scaling from blob theory to polydisperse polymer solutions.

5. Conclusions

We have explored the "universal scaling" of rheological properties of semidilute linear polymer solutions based on the "blob" model for semidilute solutions and based on the conjecture of Colby−Rubinstein for concentrated solutions.[12] Starting with nearly monodisperse polystyrene solutions where "universal scaling" has already been confirmed for the zero-shear viscosity,[3] we have tested the dynamic similarity of the frequency-dependent linear viscolelastic properties of polysty-

Table 6. Weight-Average Molecular Weights and Parameters of Two Binary Blends of PS Samples in TCP

	molecular weights and ratios			parameters of short-chain polymer					
	$M_{w,short}$ g/mol	$M_{w,long}$ g/mol	$M_{w,long}/M_{w,short}$	ν^a	$[\eta]_0{}^a$ L/g	$R_g{}^b$ nm	c^{*c} g/L	$M_wA_2{}^d$ L/g	$c_e{}^e$ g/L
blend 1	1.28×10^6	2.68×10^6	2.09	0.53	0.17	43.87	25.19	0.26	84.32
blend 2	2.68×10^6	5.56×10^6	2.07	0.53	0.26	64.90	16.29	0.40	54.52

[a] $[\eta]_0 = 4.2 \times 10^{-5} M_w^{0.59}$ (L/g).[4] [b] $R_v/R_g = 0.74$ for linear PS solutions over the range $10^5 \le M_w \le 10^{6.}$[31] Here, the viscometric radius of the polymer chain R_v is calculated as $R_v = (\{3[\eta]_0 M_w\}/\{10\pi N_A\})^{1/3}$, with N_A as Avogadro's number, and $R_g = (\{3[\eta]_0 M_w\}/\{10\pi N_A\})^{1/3}/0.74$.[3] [c] $c^* \equiv M_w/(N_A R_g^3)$. [d] $M_wA_2 = 6.5/c^*$ for PS in good solvents.[2] [e] $c_e \equiv (1/M_wA_2)n_e^{3\nu-1}$.[2,3]

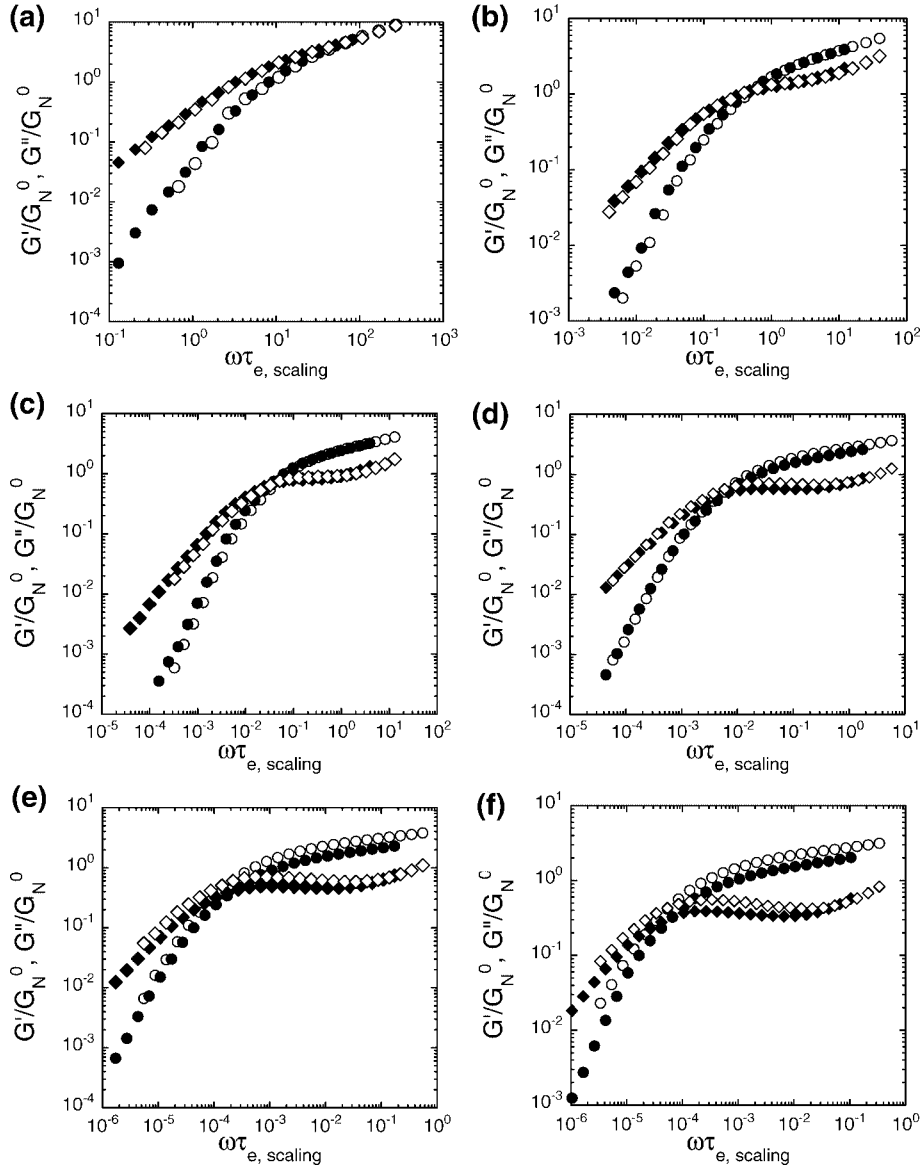

Figure 10. Superposition of linear viscoelastic properties of two binary blends of PS/TCP solutions at six different values of c/c_e: (a) $c/c_e = 0.50$, (b) $c/c_e = 1.00$, (c) $c/c_e = 1.50$, (d) $c/c_e = 2.00$, (e) $c/c_e = 2.50$, and (f) $c/c_e = 3.00$. ● and ◆, respectively, represent the normalized storage and loss moduli of the solutions with equal mass fractions of $M_{w,short} = 1.28 \times 10^6$ and $M_{w,long} = 2.68 \times 10^6$ g/mol. ○ and ◇, respectively, represent the normalized storage and loss moduli of the solutions with $M_{w,short} = 2.68 \times 10^6$ and $M_{w,long} = 5.56 \times 10^6$ g/mol. $\tau_{e,scaling}$ is based on the weight average molecular weight of long and short chains.

rene solutions, polybutadiene solutions and melts, and of binary blends of two monodisperse polystyrene solutions, as well as the shear-rate-dependent nonlinear properties of polystyrene solutions. We found that for polystyrene solutions in TCP, "universal scaling" using the de Gennes semidilute blob concept, which gives $G_N^0(\phi) = G_N^0(1)\phi^{3\nu/(3\nu-1)}$ and $\tau_{e,scaling} = (\eta_s/k_BT)R_g^3(c/c^*)^{3\nu/(1-3\nu)}n_e^2$ as scaling parameters, allows us to collapse all linear and nonlinear data, for both monodisperse and bidisperse solutions, at concentrations in the semidilute range, where the semidilute range for this polymer/solvent pair lies below a volume fraction of around 0.15, which is roughly consistent with our estimated value of the "swelling concentration" ϕ_s identified by Milner. This swelling concentration is the concentration at which the size of a correlation blob at a volume fraction $\xi(\phi)$ equals that of thermal blob l_s. For polymer chains at volume fractions below ϕ_s, there is a range of length scales over which the polymer is swollen in a good solvent, while above ϕ_s they follow random walk configurations until the length scale decreases to Kuhn segment: see Figures 5 and 6 for visual and conceptual understanding. At higher concentrations of PS

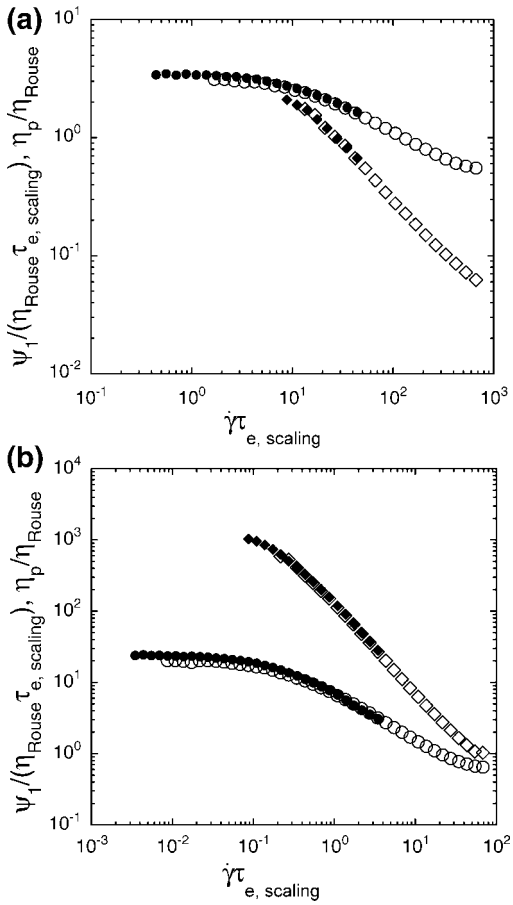

Figure 11. The same as Figure 10 except for nonlinear viscoelastic properties: (a) $c/c_e = 0.50$, and (b) $c/c_e = 1.00$.

in TCP, near the value we estimate for ϕ_s, the semidilute scaling laws based on the above formulas fail to collapse the PS/TCP data.

For $\phi > \phi_s$, we can extract the expressions for two normalizing parameters for universal scaling using the Colby−Rubinstein conjecture for Θ solutions: $G_N^0(\phi) = G_N^0(1)\phi^{1+\alpha_c}$ and $\tau_{e,scaling} = (\eta_s/k_BT)b^3N_e^2(1)\phi^{1-2\alpha_c}$, where α_c is around 1.3 for any solvent quality. While we do not have enough data for PS/TCP at concentrations above ϕ_s to test these scaling laws, we were able to use data from Colby et al.[5] for polybutadiene in phenyl octane to test and confirm these relationships for the concentrated regime over a wide range of concentrations all of the way up to the melt, because the value of ϕ_s for these polybutadiene solutions appears to be very low. Thus, scaling theory for polymer solutions is confirmed for all viscoelastic data we have examined, as long as we recognize the crossover from semidilute concentrations, where the de Gennes blob theory holds, to the concentrated regime where the Colby−Rubinstein exponent seems to be valid. The melt state is thus viewed as just a special case of "concentrated solutions", and there is no behavior we could identify that is distinctive to solutions, except possibly at the very highest frequencies, where solutions seem to show an early "upturn" in G'', before such an upturn is seen in the melts. Near the crossover between semidilute and concentrated solutions, no simple scaling is likely to apply, although if the crossover concentration were known precisely, it might even be possible to superimpose data from above the crossover onto the data below it, by using prefactors Milner obtained by imposing continuity on the scaling quantities at the crossover concentration ϕ_s.

The upshot of all of this is that rheological data obey universal scaling with a dilution exponent given by a "nearly universal" value of close to the Colby−Rubinstein value of 4/3 for all polymer solutions, except those of intermediate quality below the swelling concentration, where its value depends on the solvent quality as predicted by the de Gennes blob theory. As explained by Milner,[9] a unified theory for all regimes is obtained from the Colby−Rubinstein conjecture that the tube diameter a is proportional to the distance between "binary contacts". For the Θ solvent, or above the swelling concentration, these binary contacts are random binary "collisions" having a spatial density proportional to ϕ^2, and hence separated spatially by a distance proportional to $\phi^{-2/3}$. Below the swelling concentration in non-Θ solvents, the "collisions" are not random due to polymer repulsion. However, treating a blob as a kind of rescaled monomer, Milner surmises that there is one such "collision" per blob, which yields a tube diameter proportional to the blob size. Coincidentally, for very good solvents, this yields a dilution exponent almost identical to the value of 4/3 from the Colby−Rubinstein theory. Thus, deviations from this value of the dilution exponent are only obtained for solvents of intermediate quality in the semidilute regime.

Acknowledgment. We thank Professor Michael J. Solomon for making available to us his DAWN EOS static light scattering goniometer, and for fruitful advice on data analysis. We are very grateful to Professor Ralph H. Colby for advice regarding sample preparation, to Professors William W. Graessley and Alexei E. Likhtman for valuable discussions, and to Dr. Zuowei Wang for help in drawing Figure 6. We acknowledge support from NSF under grant DMR 0604965. Any opinions, findings, and conclusions or recommendations expressed in this material are those of the authors and do not necessarily reflect the views of the National Science Foundation (NSF).

Supporting Information Available: Sample Zimm plots of PS samples in toluene at room temperature. This material is available free of charge via the Internet at http://pubs.acs.org.

References and Notes

(1) de Gennes, P.-G. *Scaling Concepts in Polymer Physics*; Cornell University Press: Ithaca, NY, 1979.
(2) Raspaud, E.; Lairez, D.; Adam, M. *Macromolecules* **1995**, *28*, 927–933.
(3) Heo, Y.; Larson, R. G. *J. Rheol.* **2005**, *49*, 1117–1128.
(4) Solomon, M. J.; Muller, S. J. *J. Polym. Sci., Polym. Phys.* **1996**, *334*, 181–192.
(5) Colby, R. H.; Fetter, L. J.; Funk, W. G.; Graessley, W. W. *Macromolecules* **1991**, *24*, 3873–3882.
(6) Edwards, S. F. *Proc. Phys. Soc.* **1966**, *88*, 265–280.
(7) Graessley, W. W. *Polymeric Liquids & Networks: Dynamics and Rheology*; Garland Science: New York, 2008.
(8) Rubinstein, M.; Colby, R. H. *Polymer Physics*; Oxford University Press, Inc.: New York, 2003.
(9) Milner, S. T. *Macromolecules* **2005**, *38*, 4929–4939.
(10) Marin, G.; Montfort, J. P.; Monge, P. *Rheol. Acta* **1982**, *21*, 449–451.
(11) Colby, R. H.; Rubinstein, M.; Daoud, M. *J. Phys. II (France)* **1994**, *4*, 1299–1310.
(12) Colby, R. H.; Rubinstein, M. *Macromolecules* **1990**, *23*, 2753–2757.
(13) Adam, M.; Delsanti, M. *J. Phys. (Paris)* **1983**, *44*, 1185–1193.
(14) Adam, M.; Delsanti, M. *J. Phys. (Paris)* **1984**, *45*, 1513–1521.
(15) Adam, M.; Lairez, D.; Raspaud, E. *J. Phys. II* **1992**, *2*, 2067–2073.
(16) Heo, Y.; Larson, R. G. *J. Rheol.* **2007**, *51*, 1099–1100.
(17) Doi, M.; Edwards, S. F. *The Theory of Polymer Dynamics*; Oxford University Press, Inc.: New York, 1986.
(18) Ferry, J. D. *Viscoelastic Properties of Polymers*, 3rd ed.; Wiley: New York, 1980.
(19) Zimm, B. H. *J. Chem. Phys.* **1956**, *24*, 269–278.
(20) Rouse, P. E. *J. Chem. Phys.* **1953**, *21*, 1272–1280.
(21) Stepanek, P.; Perzynski, R.; Delsanti, M.; Adam, M. *Macromolecules* **1984**, *17*, 2340–2343.
(22) Noda, I.; Kato, N.; Kitano, T.; Nagasawa, M. *Macromolecules* **1981**, *14*, 668–676.
(23) Isono, Y.; Fujimoto, T.; Takeno, N.; Kaijiura, H.; Nagasawa, M. *Macromolecules* **1978**, *11*, 888–893.

(24) Plazek, D. J.; Riande, E.; Markovitz, H.; Taghupathi, N. *J. Polym. Sci., Polym. Phys. Ed.* **1979**, *17*, 2189–2213.
(25) Osaki, K.; Nishimura, Y.; Kurata, M. *Macromolecules* **1985**, *18*, 1153–1157.
(26) Osaki, K.; Takatori, E.; Tsunashima, Y.; Kurata, M. *Macromolecules* **1987**, *20*, 525–529.
(27) Fetters, L. J.; Lohse, D. J.; Richiter, T. A.; Zirkel, A. *Macromolecules* **1994**, *27*, 4639–4647.
(28) Likhtman, A. E.; McLeish, T. C. B. *Macromolecules* **2002**, *35*, 6332–6343.
(29) Larson, R. G.; Sridhar, T.; Leal, L. G.; McKinley, G. H.; Likhtman, A. E.; McLeish, T. C. B. *J. Rheol.* **2003**, *47*, 809–818.
(30) Schausberger, A.; Schindlauer, G.; Janeschitzkriegl, H. *Rheol. Acta* **1985**, *24*, 220–227.
(31) Graessley, W. W. *Polymeric Liquids & Networks: Structure and Properties*; Garland Science: New York, 2004.
(32) Larson, R. G. *Rheol. Acta* **1992**, *31*, 213–263.
(33) Pattamaprom, C.; Larson, R. G. *Macromolecules* **2001**, *34*, 5229–5237.
(34) Hayward, R. C.; Graessley, W. W. *Macromolecules* **1999**, *32*, 3502–3509.
(35) Baumgaertel, M.; De Rosa, M. E.; Machado, J.; Masse, M.; Winter, H. H. *Rheol. Acta* **1992**, *31*, 75–82.
(36) Roovers, J. *Polym. J.* **1986**, *18*, 153–162.
(37) Raju, V. R.; Menezes, E. V.; Marin, G.; Graessley, W. W.; Fetters, L. J. *Macromolecules* **1981**, *14*, 1668–1676.

MA800521G